Nondestructive Dynamic Evaluation of a Concrete Reaction Wall—Numerical and Experimental Studies

Gregory McLaskey[1] and Mary Sansalone, M.ASCE[2]

Abstract: Proper identification of the modes of vibration of a structure is crucial in order to avoid the condition of resonance under dynamic loading conditions. A combination of numerical simulation, physical experimentation, and waveform analysis was employed in order to obtain a dynamic evaluation of the reaction wall for the Network for Earthquake Engineering Simulation (NEES) large scale testing laboratory at Cornell University. The first four modes of vibration of the structure were identified, and this information is now available to researchers who design experiments that utilize the NEES facility. This paper presents the numerical (finite element) studies and a description of the impact test procedure used to excite and record the response of this massive, posttensioned, reinforced concrete structure. It also illustrates how numerical modeling aided in the design of experiments and how waveform analysis proved essential for the proper characterization of the dynamic behavior of this unusual structure.

DOI: 10.1061/(ASCE)0887-3828(2006)20:3(237)

CE Database subject headings: Post tensioning; Concrete; Nondestructive tests; Wave propagation; Numerical models; Simulation; Walls; Vibration.

Introduction

The Network for Earthquake Engineering Simulation (NEES) sponsored by The National Science Foundation consists of 15 shared experimental facilities located at universities across the country. These facilities, which include shake tables, geotechnical centrifuges, tsunami wave basins, and laboratories for large scale experimentation, are linked together electronically. The goal of the program is to provide a system of world-class laboratories where researchers can collaborate remotely and conduct research aimed at lessening the impact of earthquake and tsunami related disasters.

Cornell University's contribution to the NEES project is a large displacement test facility for studying the behavior of structures, such as buried pipelines or components of buildings and bridges, under static and dynamic loading (Jones et al. 2004). One component of the facility is a massive, reinforced concrete reaction wall, which was constructed during the summer of 2004. This wall, which is shown in Fig. 1, consists of two-dozen, hollow, reinforced concrete blocks posttensioned together with steel rods. The wall can be reconfigured to accommodate different test configurations and consists of a low wall 15 m (50 ft) long and a high wall with a maximum height of 7.3 m (24 ft). This structure provides a base and reaction wall on which to mount and test other specimens.

Current research which utilizes this facility consists of tests on buried steel pipelines and other underground lifeline structures subjected to large ground movement. Other NEES projects include experiments designed to test the seismic performance of highly ductile, above ground, bridge piles made of advanced materials. These experiments will be carried out on the upper surface of the low wall with static and dynamic lateral loads applied from the high wall. The reader may find more information regarding the Cornell NEES facility at ⟨www.nees.cornell.edu⟩.

Before the wall could be used as intended, however, an understanding of the response of the reaction wall to dynamic loading was needed so that any experiments that might be designed and carried out in the future do not excite modes of vibration in the wall itself. Gaining this understanding was the focus of the work presented in this paper. Specifically, the goal was to identify the natural frequencies and corresponding deformed shapes of the

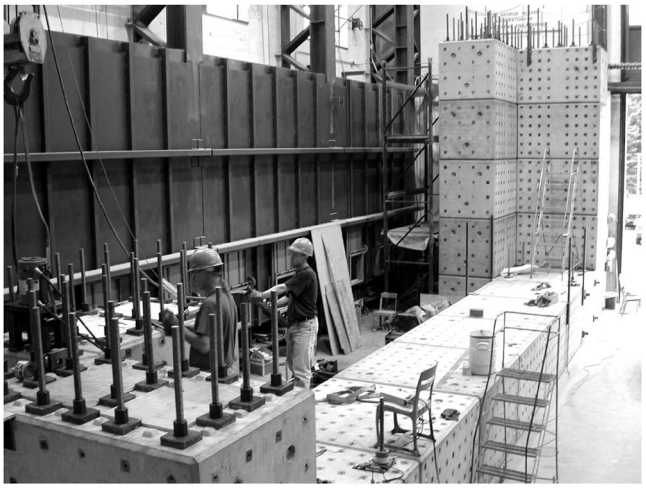

Fig. 1. Photograph of the reaction wall

[1]Undergraduate Researcher, Civil and Environmental Engineering, Cornell Univ., Ithaca, NY 14853.

[2]Professor of Civil Engineering, Dept. of Civil and Environmental Engineering, Cornell Univ., Ithaca, NY 14853.

Note. Discussion open until January 1, 2007. Separate discussions must be submitted for individual papers. To extend the closing date by one month, a written request must be filed with the ASCE Managing Editor. The manuscript for this paper was submitted for review and possible publication on March 9, 2005; approved on June 24, 2005. This paper is part of the ***Journal of Performance of Constructed Facilities***, Vol. 20, No. 3, August 1, 2006. ©ASCE, ISSN 0887-3828/2006/3-237–243/$25.00.

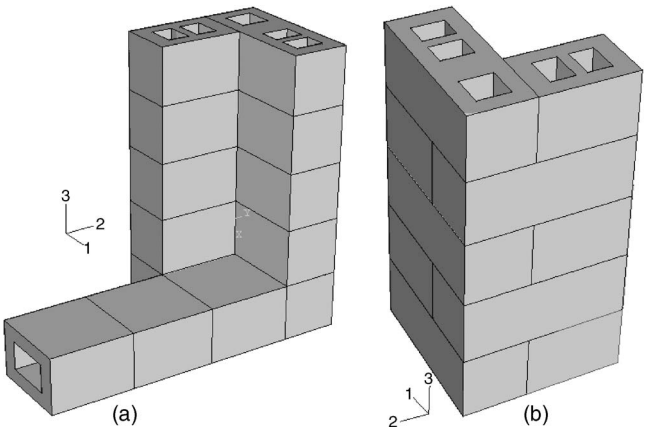

Fig. 2. Diagram depicting reaction wall geometry: (a) low wall and high wall; (b) high wall

high wall. This paper presents the results of both the numerical and experimental studies and demonstrates how the two approaches were used in a complementary way to gain the desired understanding.

Background

The high wall has an "L" cross section as shown in Fig. 2. In its current configuration, the wall is approximately 6 m tall and 3 m wide and is made up of five interlocking layers consisting of a large block 3.05 m by 1.22 m by 1.22 m (10 ft×4 ft×4 ft) and a smaller block 1.83 m by 1.22 m by 1.22 m (6 ft×4 ft×4 ft). The five layers in the high wall are posttensioned together with high strength steel rods and the bottom layer is also posttensioned to the low wall in two directions. The structure is secured to the laboratory floor with 12 rock anchors, four of which are under the high wall.

The reaction wall is a type of structure not commonly built and analyzed, and therefore there were no documented cases with which to compare or from which to predict dynamic behavior. In addition, the L-shaped wall geometry does not lend itself to solutions derived for more conventional structures like beams, frames, or plates. In fact, no accurate analytical derivations for calculating the natural frequencies of the wall were available, and thus numerical modeling (finite element) was used in conjunction with experiments to understand the dynamic response of the wall. Impact tests were used to excite and record the acceleration of the structure. Such tests use a mechanical elastic impact (such as from a hammer) to generate stress waves containing a range of frequencies (Malhotra and Carino 2004). If the frequencies in the stress waves match the frequencies of the natural modes of vibration of the wall, these modes will be excited. The resulting vibrations can be recorded and analyzed.

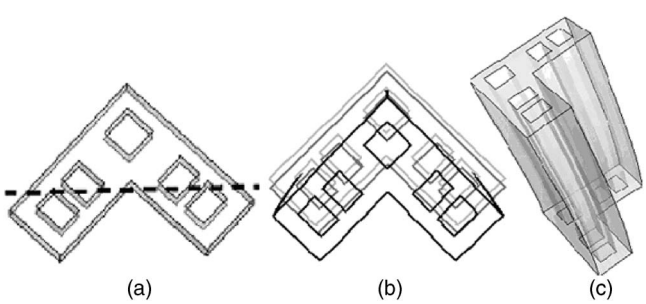

Fig. 3. Modal shape 1: (a) axis of bending; (b) translation of the cross section during motion; and (c) isometric view of deformed shape

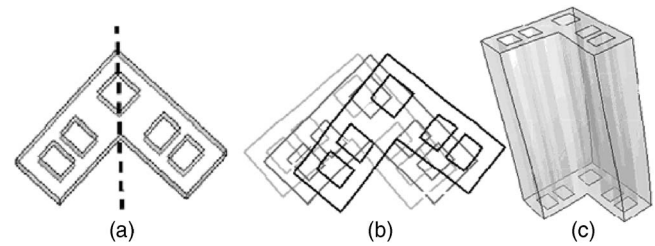

Fig. 4. Modal shape 2: (a) axis of bending; (b)translation of the cross section during motion; and (c) isometric view of deformed shape

Numerical Studies

Before the physical tests could be designed, a preliminary estimate of the dynamic behavior of the wall was needed. Estimates of modal frequencies were needed so that the proper impactor size, the length of the recorded signal, and the sampling rate could be determined. In addition, an estimate of deformed shapes was required in order to design the optimum test configurations and sensor locations to best isolate the motion associated with each frequency.

For the initial analysis, simplifying assumptions were made. The modular, reinforced concrete, posttensioned wall was modeled as a continuous structure composed of a linear elastic, homogenous material with estimates of elastic modulus and density consistent with those of heavily reinforced, high strength concrete. Full fixity of the wall to the floor was assumed, although the actual wall is secured to the floor and low wall with eight rock anchors. Thus this initial model had a fixity condition that was somewhat more rigid than the actual situation. The first four modes are shown in Figs. 3–5, and their frequencies are listed in Table 1. Eigenvalue solutions were used to obtain modal shapes and their corresponding frequencies. The finite element code, ABAQUS/CAE 6.4 (2003), was used to perform the numerical analyses.

The first deformed shape found from the eigenvalue analysis was that of bending. Fig. 3(a) shows the cross section of the high wall and the neutral axis about which bending occurs. Fig. 3(b) shows the motion of the cross section during vibration. Fig. 3(c)

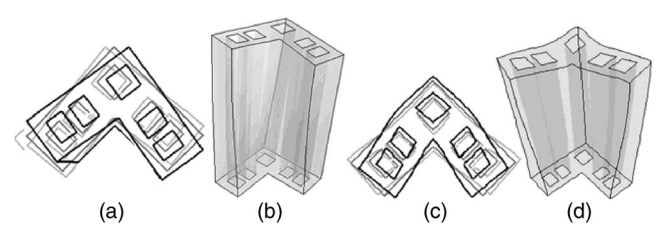

Fig. 5. Modal shapes 3 and 4: (a) motion due to Mode 3; (b) isometric view of deformed shape corresponding to Mode 3; (c) motion due to Mode 4; and (d) isometric view of deformed shape corresponding to Mode 4

Table 1. First Four Modes of Vibration

Mode	Shape	Frequency from FEA (Hz)
1	Pure bending	35
2	Side side twist	42
3	Torsion	68
4	Flange motion	110

shows an isometric view of the high wall with a magnified deformed shape. For the purposes of this paper, this shape will be referred to as deformed shape 1, "pure bending."

The second shape found from the numerical analysis, deformed shape 2, is shown in Fig. 4. This shape is produced primarily from bending, although some twisting is also present. Once again, the neutral axis about which deformation primarily occurs is depicted in (a), while the motion of the cross section is shown in (b), and an isometric view of the deformed shape is shown in (c). Deformed shape 3 is depicted in Figs. 5(a and b) and deformed shape 4 is shown in Figs. 5(c and d). Deformed shape 3 is almost purely torsional while deformed shape 4 contains motion of the flanges of the "L" cross section.

When planning the impact tests, three additional test parameters needed to be considered: location of the mechanical impact, location of the sensors with respect to the cross section of the wall, and the direction of the sensors' orientation. After inspecting the four primary deformed shapes, three test configurations and two sensor locations were chosen. These are shown in Fig. 6. All impact and sensor locations were at the top of the wall. Test Configuration 1 [Fig. 6(a)] was designed to record predominantly the motion of the first mode of vibration ("pure bending"). Test Configuration 2 [Fig. 6(b)] was designed to record the motion of all of the four primary modes of vibration. Test Configuration 3 [Fig. 6(c)] was designed to record predominately the motion of the third and fourth modes of vibration. Of the two sensor locations, Sensor Location 1, close to the center of rotation of the wall, was designed to isolate motion due to translation of the top of the wall (shapes 1 and 2) and not record motion due to rotation of the structure. Sensor Location 2, on the end of the leg of the "L" cross section of the wall was designed to record motion from both the translation and the rotation of the structure.

Prior to performing laboratory tests, impact tests were simulated using an implicit, dynamic finite element analysis in order to confirm that the test configuration and sensor location would yield the desired information. Elastic impact was simulated as pressure on a 0.2 m by 0.2 m portion of the surface of the wall with a force-time function in the shape of a half sine curve with a duration of 0.003 s. Such an impact generates stress waves with significant energy in frequencies up to about 400 Hz, which was more than sufficient to excite the first four modes of vibration of the wall (Sansalone and Streett 1997). The response was obtained

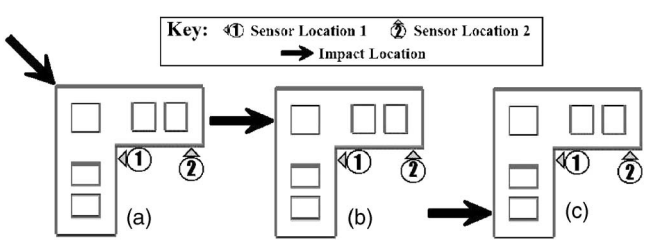

Fig. 6. Test Configurations: (a) 1; (b) 2; and (c) 3

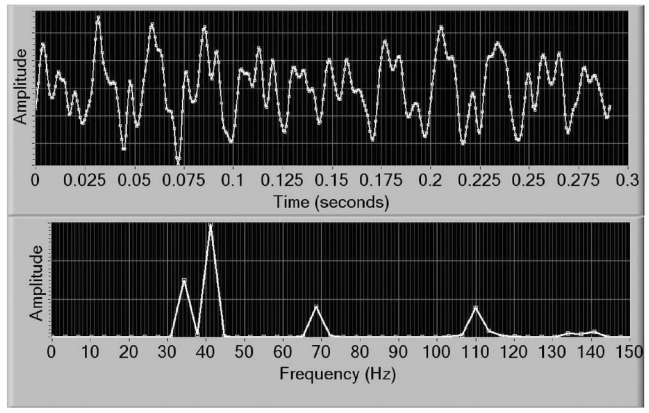

Fig. 7. Waveform and spectrum obtained from numerical simulation of impact Test Configuration 3 Sensor Location 3

by analyzing the displacement of the nodes located on the surface of the numerical model at points where sensors were to be located for a duration of 0.3 s.

Figure 7 shows results from a typical analysis. In this case, the results are for Test Configuration 3, Sensor Location 2. The upper graph shows the displacement of the top corner of the wall (in the direction normal to the surface of the wall) over time. The lower graph is an amplitude spectra obtained by taking a fast Fourier transform of the time domain waveform. The peaks in the spectrum correspond to the dominant periodicities on the waveform. The first four peaks occur at frequencies, which, from least to greatest correspond to deformed shapes 1–4, respectively. These frequencies match those predicted by the eigenvalue analysis. These simulations verified that the chosen test configurations and sensor locations were adequate for the retrieval of all of the desired information and that experimentation could commence.

Experimental Studies

In the experiments, the impact was made by a massive steel slug of about 360 kg (800 lb). The duration of the impact was approximately 0.006 s which was sufficient to generate stress waves with significant energy in frequencies up to 200 Hz. The response of the structure was recorded using two, high sensitivity, general purpose accelerometers with a frequency range of 1–4,000 Hz. These were aligned such that acceleration was recorded in both the N-S and E-W directions. Using a coordinate transform function, the acceleration in any direction could be attained. The response was recorded at a rate of 2,000 samples per second for 7 s with a PC-based data acquisition system. The 7 s record length was sufficiently long to capture the dynamic response of interest. The resolution in the amplitude spectrum was 0.14 Hz. The test setup is shown in Fig. 8.

Of primary importance is the identification of Mode 1, the fundamental and most important mode of vibration of the structure. Test Configuration 1 was designed for this purpose. Fig. 9 shows the acceleration recorded at Sensor Location 1 in the N-S direction. The response is shown in both the time and frequency domains. The time domain waveform [Fig. 9(a)] is sinusoidal in nature, indicating that it is dominated by a single frequency. The spectrum [Fig. 9(b)] exhibits one distinct peak at 15.75 Hz.

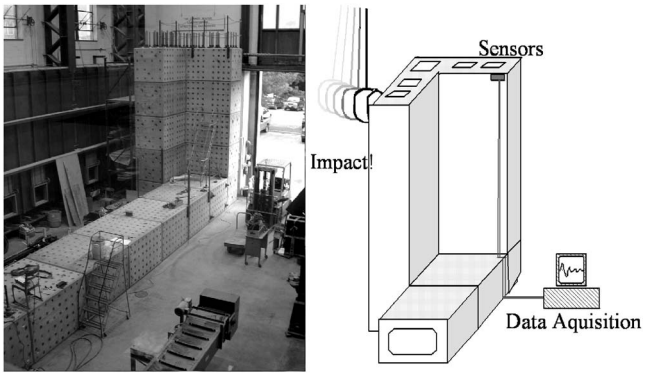

Fig. 8. Photograph of reaction wall and diagram of testing configuration

In addition to its presence in Test Configuration 1, if the 15.75 Hz frequency truly is the fundamental mode of vibration of the structure, it should also be excited by the other test configurations as well. Fig. 10 shows the response of the wall for Test Configuration 2 in which all modes of vibration are excited. The response shown is acceleration in the N-S direction. As predicted, the 15.75 Hz signal is the dominant signal in this direction.

To identify Mode 2 the motion of the wall in the E-W direction was analyzed. Fig. 11 shows the response of the wall from testing Configuration 2 measured at Sensor Location 1 in this direction. As predicted by the numerical analysis, two distinct frequencies are present. There is a distinct peak at 15.75 Hz corresponding to Mode 1, and a peak at 21.5 Hz corresponding to Mode 2. The 21.5 Hz frequency is present at other sensor locations and in different testing configurations as well, but it is strongest in the E-W direction. This evidence strongly supports the conclusion that 15.75 Hz and 21.5 Hz are in fact the natural frequencies corresponding to Modes 1 and 2 and that their deformed shapes are very similar to those predicted by the numerical study.

Proper identification of Modes 1 and 2 are all that is absolutely necessary to satisfy the needs of the NEES laboratory, but further investigation of Modes 3 and 4 provided useful insight into both the behavior of the wall and the robustness of the numerical model.

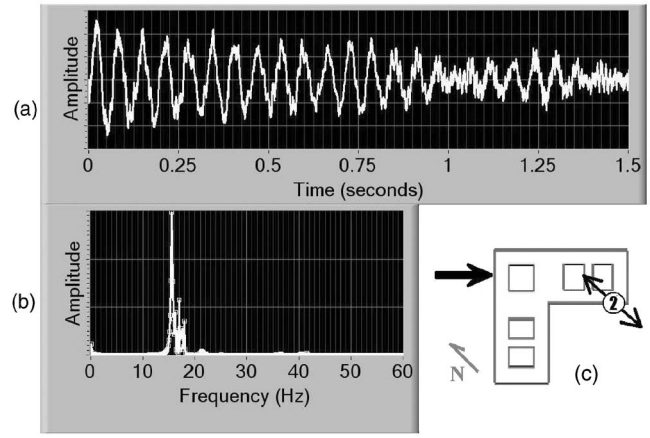

Fig. 10. Results obtained from Test Configuration 2, Sensor 2: (a) waveform; (b) spectrum; and (c) schematic showing sensor location and orientation

The amplitude spectra corresponding to two different directions of testing Configuration 2 are shown in Fig. 12. If the predictions made by the numerical study are correct, Modes 3 and 4 should be present in the direction perpendicular to the flange of the "L" cross section of the wall at Sensor Location 2 [shown in Fig. 12(a)], but there should be no motion in the direction parallel to the flange of the "L" cross section of the wall in the same location [shown in Fig. 12(b)]. As expected, two small peaks, located at 36 and 42 Hz, appear in (a) but not in (b). These two frequencies are most likely produced by Modes 3 and 4.

Without more extensive physical testing it is difficult to distinguish between modal shapes 3 and 4, or to prove conclusively that these frequencies do in fact correspond to the predicted shapes. There are, however, a few simple checks that support this conclusion. First, due to the fact that these modal shapes do not produce gross translation of the center of the cross section of the wall, these frequencies should not be present at Sensor Location 1 in any direction. A reexamination of Fig. 11 shows that this is in fact the case. In addition, the frequencies corresponding to Modes 3 and 4 should be very prevalent in Test Configuration 3, which was designed to excite and record motion due to these modes of vibration.

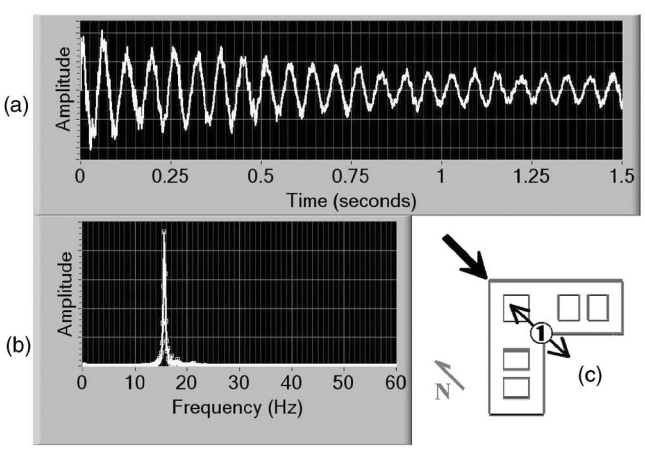

Fig. 9. Results obtained from Test Configuration 1, Sensor 1: (a) waveform; (b) spectrum; and (c) schematic showing sensor location and orientation

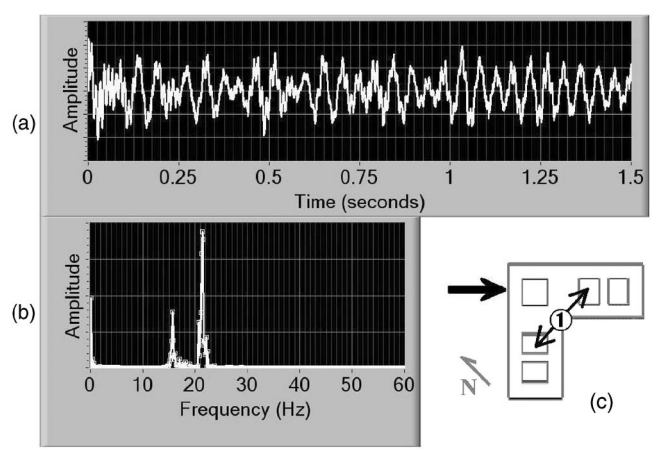

Fig. 11. Results obtained from Test Configuration 2, Sensor 1: (a) waveform; (b) spectrum; and (c) schematic showing sensor location and orientation

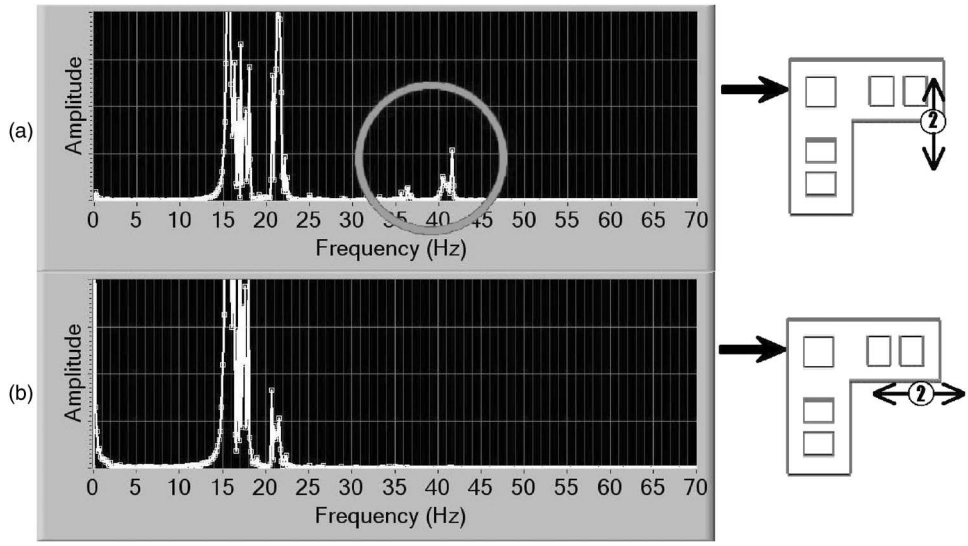

Fig. 12. Test Configuration 2: (a) Modes 3 and 4 are present; (b) Modes 3 and 4 are absent

The response from this testing configuration is shown in Fig. 13. It shows a dominant 41 to 42 Hz peak and a very low amplitude response at 36 Hz. Upon closer examination of the waveform at different times over the period of response, one can more clearly distinguish between the two frequencies. As shown in Fig. 14, during the first second after impact [Fig. 14(a)] the 41 to 42 Hz response initially dominates. However, as shown in the spectra corresponding to the time domain response from 3 to 4 s after impact [Fig. 14(b)], and the response from 5 to 6 s after impact [Fig. 14(c)], as the 41 to 42 Hz frequency decays, the 36 Hz response becomes easier to see. Similar results are found from a careful examination of the waveform obtained from Test Configuration 2. From this evidence, it is highly probable that these two frequencies are very similar to those predicted by the numerical model, and it is likely that the 36 Hz signal is due to Mode 3 and the 42 Hz signal is due to Mode 4.

Comparison of Frequencies Obtained from Numerical and Experimental Studies

After the identification of the four modal shapes it is useful to compare the frequencies predicted using the numerical model with those found from the physical test results. Table 2 shows both numerical and experimental results and the ratio of these two frequencies for each mode. The numerical test results produced notably different frequencies that are approximately twice that of those obtained experimentally for modes 1–3.

In order to explore the source of this difference between experimental and numerical results, all variables which might affect the natural frequencies of the structure were identified. Vibration of a continuous cantilevered beam, or wall in this case, depends on its material properties (elastic modulus and density) and its slenderness (the height and bending moment of inertia) (Chopra

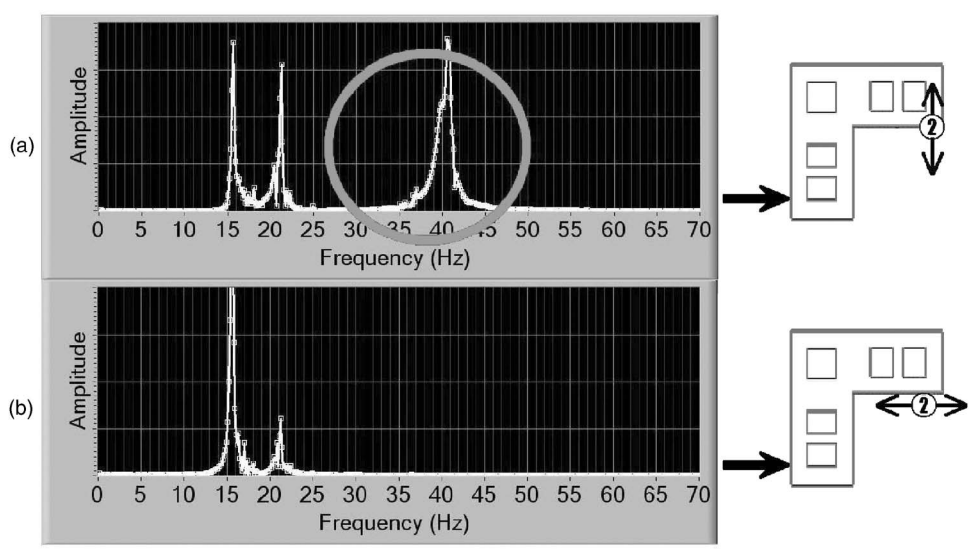

Fig. 13. Test Configuration 3: (a) Modes 3 and 4 are present: (b) Modes 3 and 4 are absent

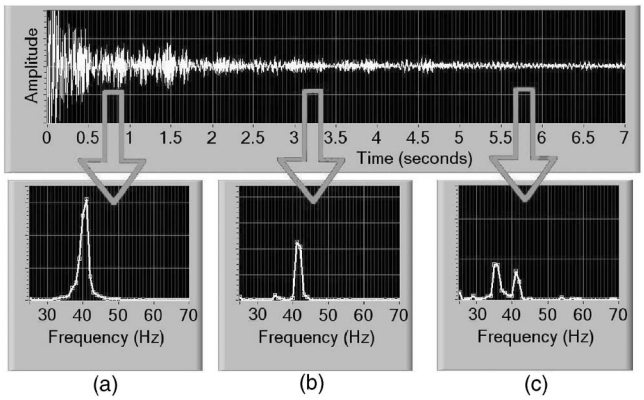

Fig. 14. Waveform examination [of the results shown in Fig. 13(a)]: frequency spectra corresponding to 1 s of the waveform (a) immediately after impact; (b) 3 to 4 s after impact; and (c) 5 to 6 s after impact

2001). In addition to these factors, the boundary conditions at the base of the wall and the assumption that the wall behaves as a continuous beam instead of an assembly of tensioned blocks were other possible sources of error. In order to check the significance of these factors, the numerical model was systematically altered in order to determine if a change in any of these parameters or features had a significant effect on the results. It was found that changes in material properties, boundary conditions, and friction and interaction characteristics between the tensioned blocks produced no significant changes in the natural frequencies obtained from the numerical model. In order to yield frequencies as low as those obtained from physical testing, the wall would have to be unrealistically flexible or possess a substantially different geometry. For example, the modulus of elasticity of the model would have to be reduced by a factor of 4 to produce a 50% reduction in the frequency of Mode 1. As slenderness was the only remaining factor, it seemed that something in the physical makeup of the wall was causing it to behave as if it were effectively more slender than it initially appeared to be.

The most significant difference between the numerical model and the actual wall is that the model assumes that each block comprising the wall possesses perfect geometry while the actual blocks making up the wall are imperfect. The faces of the blocks are not perfectly smooth, nor are they perfectly flat. Match cast concrete blocks were not financially feasible, and due to the way the blocks were cast, most of them have slightly convex surfaces. Even if this convexity only protrudes a millimeter or two, it would be enough to change the way loads are distributed from block to block when the structure is tensioned. As shown in Fig. 15, this convexity of the blocks would reduce the effective width of the wall, making the structure more slender and accounting for the lower frequencies.

Table 2. Comparison of Frequencies Obtained from Physical Tests and Numerical Simulation

		Frequency		
Mode	Shape	From FEA (Hz)	From experimental testing (Hz)	Ratio
1	Pure bending	35	15.75	2.2
2	Side side twist	42	21.5	2.0
3	Torsion	68	36	1.9
4	Flange motion	110	42	2.6

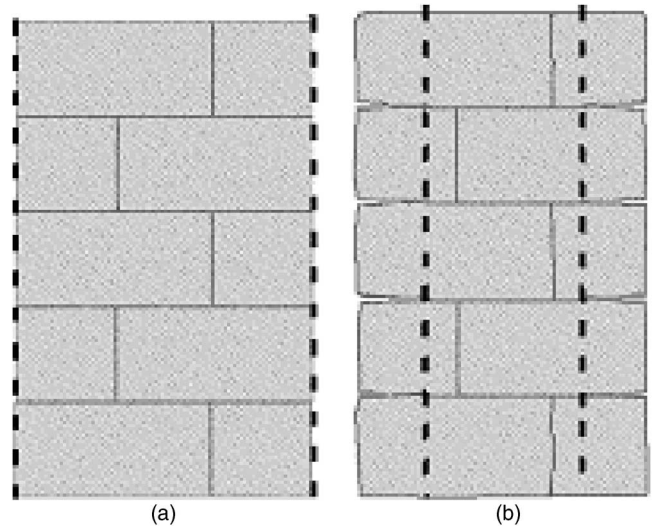

Fig. 15. Block convexity effectively reduces the cross section of the wall: (a) flat blocks; (b) convex blocks

Approximate calculations indicate that only a 25% decrease in the slenderness of the wall would be required to achieve the observed 50% reduction in the frequency of the first mode of vibration. Additionally, because the poor block to block contact is most prevalent at the edges of the structure and the blocks are hollow at the center, the convexity of the blocks dramatically reduces the effective cross-sectional area of the wall. It is entirely possible that a 25% reduction in the effective cross section of the wall has occurred at one of the interfaces between layers of blocks. Finally, the interlocking nature of the wall also lends itself to further complications associated with imperfect block geometry. Any one of many imperfect interfaces between blocks, or between the blocks and the floor could cause the observed reduction in the frequences of the wall.

Conclusion

Though the task of evaluating the massive NEES reaction wall was not straightforward, by combining numerical modeling and physical testing, four modal shapes and their corresponding frequencies were identified, and insights into the dynamic behavior of the wall were attained. This information will now be available to those who design experiments that make use of the NEES facility.

The numerical models proved to be a valuable tool in evaluating the performance of the existing reaction wall, providing understanding, aiding in the design of physical tests, and reducing the amount of testing required for the identification of the natural frequencies and modal shapes of the wall. Without the insights gained from the numerical models, the number of sensors needed and the amount of physical testing necessary to fully characterize the dynamic response of the wall could easily have been overwhelming. Finally, by comparing the results obtained from the numerical model (idealized case) to physical results (real world response) and carefully trying to reconcile the differences, conclusions could be drawn about how imperfections in the construction of the wall affect its dynamic response.

Acknowledgments

The writers would like to gratefully acknowledge Dr. Keith Kesner, NEES research associate and designer of the wall, Mr. Timothy Bond, manager of Cornell's Civil Infrastructure Laboratory, Professor Harry Stewart, co-PI for the Cornell NEES project, and Mr. Brett Shelton, NEES Project Equipment Technician, for their help with the physical testing and data acquisition system. This work was funded in part by a grant from the Cornell College of Engineering Learning Initiatives for Future Engineers (LIFE), a program designed to provide research opportunities to undergraduates.

References

ABAQUS/CAE users manual; Getting started with ABAQUS version 6.4. (2003). Abaqus Inc., Pawtucket, R.I..

Chopra, A. K. (2001). *Dynamics of structures*, Prentice-Hall, Englewood Cliffs, N.J., 635–638.

Jones, S. L. et al. (2004). "Soil-structure interaction facility for lifeline Systems." *Proc., 13th World Conf. on Earthquake Engineering*, Vancouver, B.C., Canada, Paper No. 1621.

Malhotra, V. M., and Carino, N. J. (2004). *Handbook on nondestructive testing of concrete*, 2nd Ed., CRC Press, Boca Raton, Fla. 14.1–34.

Sansalone, M. J., and Streett, W. B. (1997). *Impact echo: Nondestructive evaluation of concrete and masonry*, Bullbrier Press, Ithaca, N.Y., 31.